Jour. of the KGS, Vol. 21, No. 7. September 2005, pp. 43~54

Behaviour of Leaking Tunnels under Unconfined Flow Condition

비구속 흐름조건하에 있는 배수형 터널의 거동

Shin, Jong-Ho[1] 신 종 호

요 지

지하수위 아래에서의 터널굴착은 지하수 영역의 변화를 초래하게 되고, 지하수의 공급이 충분하게 이루어지지 않는 경우 자유수면의 하강현상이 발생하게 된다. 이러한 거동을 수치 해석적으로 모사하기 위해서는 자유수면위의 불포화토 거동을 포함하는 자유수면의 변화를 고려하기 위한 복잡한 해석 알고리즘을 채택하여야 하고, 불포화토의 수리거동을 포함하므로 통상 구속흐름조건으로 가정하여 해석하게 된다. 그러나 이 방법은 실제 많은 상황에서 발생하는 지하수위 저하를 고려하지 못하며 지하수위 저하가 터널 및 주변지반의 거동에 어떠한 영향을 미치는지 파악하기 어렵다. 본 연구에서는 비구속 흐름조건하의 지하수위 아래 배수형 터널을 건설하는 경우 지하수 영역의 변화와 이 변화가 터널과 지반에 미치는 영향을 수치 해석적 모델링 방법을 통하여 파악하고, 이를 통상적 해석방법인 구속조건의 흐름과 비교 고찰하였다. 해석결과 지하수위 변화는 지표, 특히 지하수위 상부의 거동에는 지대한 영향을 미칠 수 있지만 터널라이닝 거동은 구속흐름의 경우와 거의 차이가 없는 것으로 나타났다.

Abstract

Tunnelling in a water bearing soil may cause draw-down of ground water table. Modelling of this problem requires considering the change of phreatic surface including the stress constitutive relationship for an unsaturated soil. However, it is normally assumed that ground water is confined. Numerical formulation of coupled behavior considering phreatic surface is described and implemented into computer program. Influence of unconfined flow on tunnel and ground is thoroughly investigated and compared with that of confined flow condition. It is identified that ground and lining behaviour below phreatic surface is almost the same as that under confined flow conditions, however, there is considerable difference in ground behaviour above phreatic surface. It is generally concluded that the assumption of confined flow is acceptable in terms of lining design.

Keywords : Coupled analysis, Leaking tunnel, Phreatic surface, Unconfined flow

1. Introduction

In dealing tunnelling problem, it is often assumed that hydraulic boundary condition is confined. This assumption for confined flow could be valid as long as the water table is not drawn down by the existence of the tunnel. However, for soils with high void ratio and low specific storage capacity of water, where permeability and recharge are insufficient to maintain the flow without a reduction in the piezometric level above tunnel, it is unlikely that the initial conditions could be maintained for long time once the tunnel is excavated. A transient flow, therefore, will develop with declining water table. Consequently, the completed tunnel will act as a transient drain. This type of flow can be termed as unconfined flow.

When tunnelling in a water bearing soil causes draw-

1 Member, Assistant Prof., Dept. of Civil Engrg., Konkuk Univ., jhshin@konkuk.ac.kr

down of ground water table, soils above phreatic surface may experience desorption process as illustrated in Figure 1 (a). Once de-saturation occurs, suction will be developed in a dewatered zone. The volume of the pores occupied by water and the area of water available for flow decrease with decreasing saturation as presented in Figure 1 (b), and the permeability of the soil also decreases with decreasing saturation in the manner shown in Figure 1 (c).

In transient flow, phreatic surface will appear and vary with time until a hydraulic equilibrium is reached. In the region above phreatic surface, a soil which is initially saturated, becomes unsaturated. If unsaturated flow occurs, pore water pressure, permeability and degree of saturation interact. Coupling of pore water pressure and permeability requires a solution which utilizes the Laplace equation. Consequently, the modelling of phreatic surface problem involves the modification of continuity equation considering changes of ground water table. Shin et al (2002) investigated the long-term effect of ground water on tunnel. However, in their study the behavior of ground and tunnel lining due to unconfined flow condition has not been clearly identified.

2. Formulation and FE Implementation

The modelling of tunnelling under unconfined flow condition may require the stress constitutive relationship for a unsaturated soil which is above phreatic surface. In this study, the draw-down of phreatic surface is simulated using Biot's (1941) consolidation theory with the modification of continuity equation.

However, Biot's theory assumes that the soil is saturated. Accordingly, it is assumed that the soil between the initial phreatic surface and current phreatic surface is saturated. It is assumed that the degree of saturation is sufficiently high so that the air bubbles are dissolved in water so that the effective stress principle is valid. This condition prevails at degree of saturation greater than about 85% (Sparks, 1963; Barden, 1965).

The phreatic surface problem includes some extension of Biot's theory which makes possible finite element analyses of the consolidation of soil masses above phreatic surface. According to Childs and George (1950), Darcy's law, which states that the velocity of flow is proportional to the hydraulic head, is applicable to both saturated and unsaturated soil media, i.e. above and below ground water table:

$$v_i = k_{pf}\frac{dh}{dx_i} \tag{1}$$

where v_i is the seepage velocity in the x_i-direction, k_{pf} is the coefficient of permeability expressed as a function of suction pore water pressure, and h is the total hydraulic head.

Figure 2 (a) illustrates the variation of phreatic surface with time. Assuming that the flow is governed by the usual Laplace equation, the boundary conditions along the phreatic surface can be expressed by two terms; the energy conservation equation:

$$h = h_E \tag{2}$$

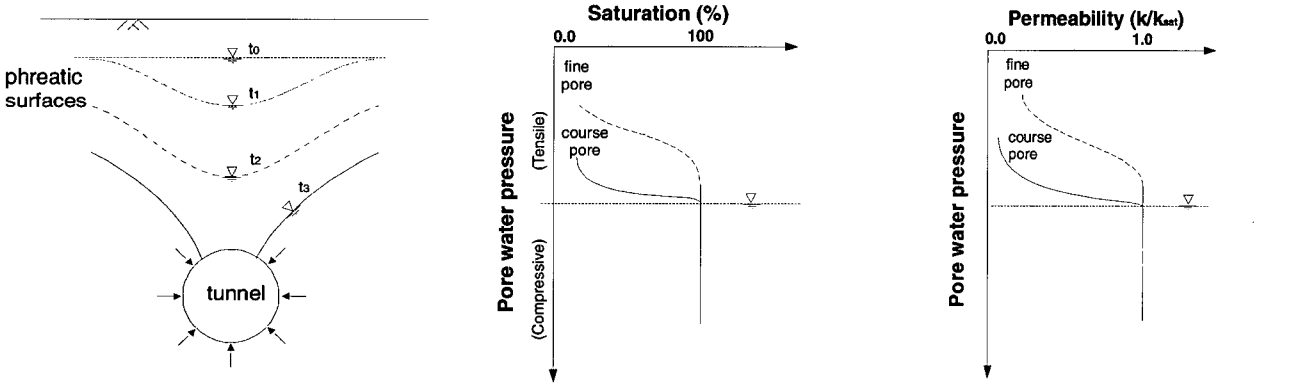

(a) Phreatic surface (b) Saturation above the phreatic surface (c) Permeability above the phreatic surface

Fig. 1. Phreatic surface problem due to tunnelling

where h is the total head and h_E is the elevation head, and the continuity equation:

$$v_n = -k_{pf}\frac{dh}{dh} = \frac{dh'}{dt} \tag{3}$$

where v_n is the seepage velocity normal to the phreatic surface and h is the effective seepage length normal to phreatic surface, i.e. $dh = n_e\, dh\cos\theta$ in which n_e is the effective porosity as shown in Figure 2 (b) and θ is the angle between the phreatic surface segment and the x -direction. The satisfaction of these mixed boundary conditions can be obtained in two steps. Firstly, using Equation (2), the location of phreatic surface where the pore water pressure head is zero can be determined. Secondly, along the phreatic surface the flow condition in Equation (4) is imposed:

$$-k_{pf}\frac{dh}{dn} = \frac{n_e h_{FS}\cos\theta}{dt} \tag{4}$$

where h_{FS} is the total head at the phreatic surface, n is

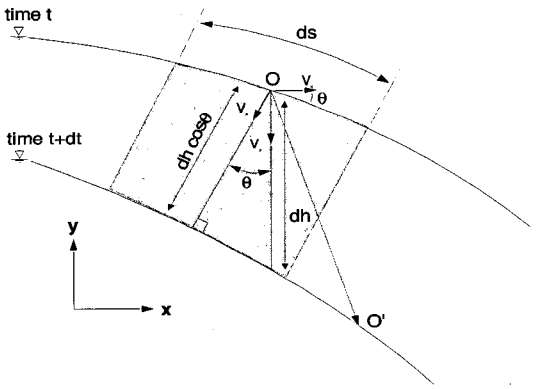

(a) Change of phreatic surface due to flow into tunnel

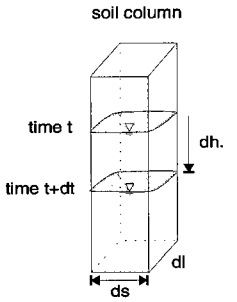

S_y = Δq / V
= (dh ds dl n_e) / (dh ds dl)
= n_e

(b) Specific yield (S_y) and effective porosity (n_e)

Fig. 2. Schematic diagram for phreatic surface problem

porosity and t is time. Then the modified finite element equation can be obtained by using the normal finite element procedure. The virtual work expression of continuity can be rewritten by imposing the phreatic surface boundary condition as:

$$\int_V \Delta h^T(k_{pf})\Delta p\, dV = -\int_S P n_e \frac{dh_{FS}}{dt}\cos\theta\, dS \tag{5}$$

where S is the phreatic surface contour and V is the volume influenced by the draw-down of ground water table ($=dnds$). Finite element approximations can be incorporated as, $p = N_p\ p_i$ and $h = N_p h_i$, where N_p is the pore water pressure shape function.

However, phreatic surface problem can not be solved straightforward. It is required to know $\{h_{FS}\}$ at $t+\Delta t$. Using iterative scheme, $\{h_{FS}\}$ at $t+\Delta t$ can be partitioned as:

$$\begin{aligned}\left\{h_{FS}^{t+\Delta t}\right\}_j &= \left\{h_{FS}^{t+\Delta t}\right\}_{j-1} + \{\Delta h\} \\ &= \left\{h_{FS}^{t+\Delta t}\right\}_{j-1} + \frac{1}{\gamma_w}\{\Delta p\}\end{aligned} \tag{6}$$

where j is the jth iteration, $\{\Delta h\}$ is the change of hydraulic head from the $(j-1)$th iteration to the jth. By considering the continuity equation, a new approximate global finite element coupled equation can be obtained.

Iterative scheme is necessary and therefore, the Modified Newton Raphson method is applicable to solve the coupled equation. The solution procedure to determine the phreatic surface is similar to those adopted for the nonlinear problems. It is required to know the location of the phreatic surface at each iteration. This can be achieved by imposing the boundary condition on the phreatic surface so that the total water head is equal to the elevation head.

$$h - h_E = \sum_{i=1}^{n} N_{p,i}(\xi,\eta)(h_i - h_{Ei}) = 0 \tag{7}$$

where n is the number of node in an element. $N_{p,i}(\xi,\eta)$ is the pore water pressure shape function expressed in the natural coordinates, h_i is the approximated total head and h_{Ei} is the elevation head at the phreatic surface. By solving the Equation 7, the natural coordinates (ξ,η) along the free surface are obtained and hence the global coor-

dinates (x, y) can be found. Once the location of the phreatic surface is determined, the steps are taken into to identify whether a Gauss point lies above or below the phreatic surface and then reduce seepage by reducing the permeability for the Gauss points above the phreatic surface. This process continues until the change in pore pressure (or total water head) at each node is smaller than a given convergence tolerance. This numerical process is implemented into Imperial College Finite Element Program (ICFEP) and used for the analyses presented in this study.

To consider the reduction of seepage above phreatic surface, it is necessary to redefine the coefficient of permeability so that the flow reduces. The 'permeability function' is commonly used to represent the relationship between the coefficient of permeability and soil suction (Fredlund, 1997) as shown in Figure 3 (a). Simplified empirical equations are frequently used in engineering practice. A linear relationship between log suction and permeability is assumed in this study as shown in Figure 3 (b). This permebility function was used in the analyses presented here and can be expressed in the form:

$$\log k = \log k_{\max} - \frac{(p-p_1)}{(p_2-p_1)} \log \frac{k_{\max}}{k_{\min}} \qquad (8)$$

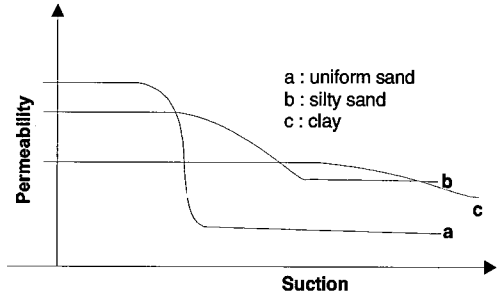

(a) relationship between permeability and suction

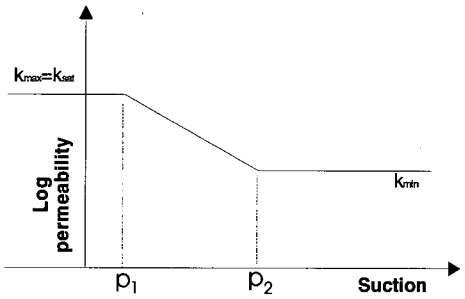

(b) Computer model for permeability function

Fig. 3. Schematic diagram for unsaturated soil behaviour (Freeze et al., 1979)

where k and p are the coefficient of permeability and corresponding suction pressure respectively, $k_{\max}$ is the coefficient of permeability for a saturated soil, $k_{\min}$ is the minimum coefficient of permeability for an unsaturated soil, p_1 is the pore pressure at which permeability begins to change, and p_2 is the suction at which permeability completes its change.

However, as coupled analysis scheme is adopted in this study, another consideration of the effect of suction on effective stress should be taken. It is known that void ratio decreases with the increase in suction to a certain point termed shrinkage limit. Beyond shrinkage limit, suction does not cause any further volume change (Toll, 1995). This behavior is incorporated in this study.

Validation and Parametric Study

As there is no closed form solution for coupled phreatic surface problem, performance of the scheme used for phreatic surface change was checked by performing the steady state seepage analysis for the known square earth dam problem as shown in Figure 4. A steady state seepage solution can be simply obtained by giving the soil fictitious linear elastic properties and applying sufficient displacement constraint to prevent rigid body motion. The

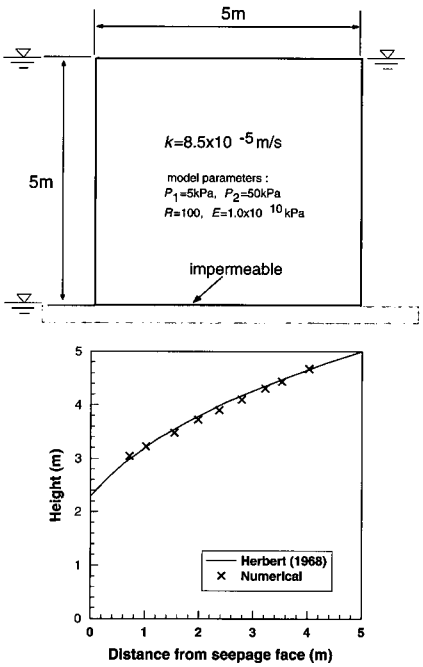

Fig. 4. Validation of phreatic surface problem

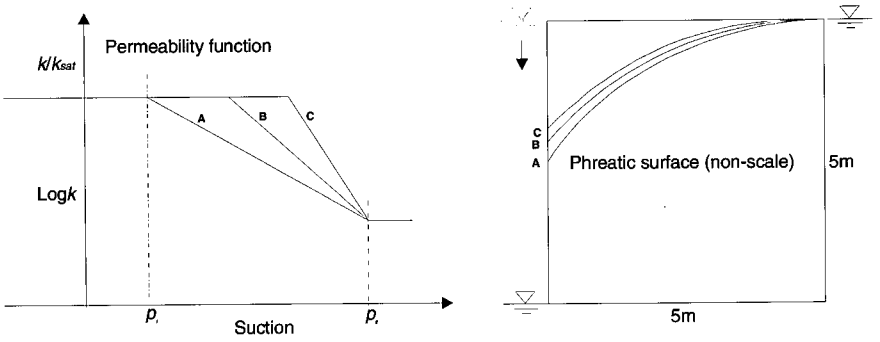

(a) Effect of p_1

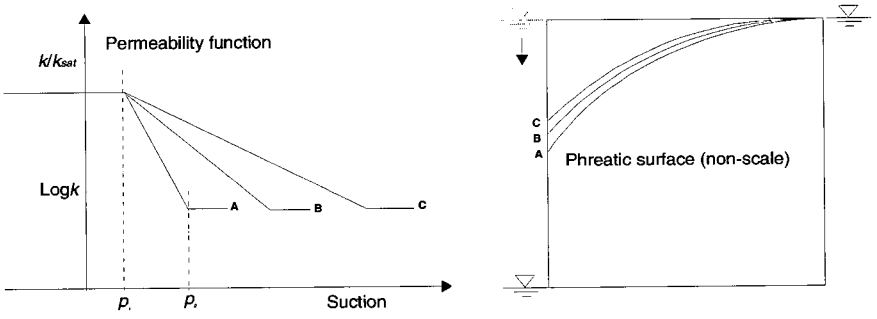

(b) Effect of p_2

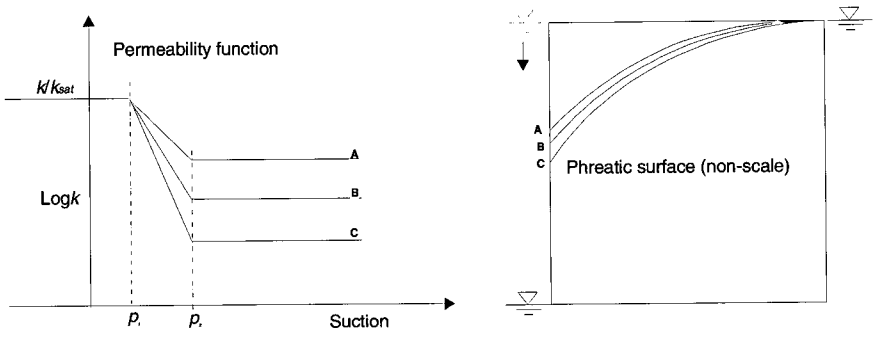

(c) Effect of R (k/k_{sat})

Fig. 5. Parametric study on permeability function

effect of model parameters of permeability function was investigated by carrying out seepage analyses for the square dam problem and the results are also presented in Figure 5.

3. Tunnel Model

This study is mainly concerned with the geotechnical aspects associated with unconfined flow. The tunnel to be analysed was adopted from one of London Underground tunnels. (Barratt *et al.*, 1976 Bowers *et al.*, 1996). A single circular tunnel with an outside diameter of 4 m was modelled. The tunnel lining was modelled using solid elements with thickness of 0.3 m. Soil and tunnel profiles for the analyses are shown in Figure 6. Tunnels at three different depths are considered: 10 m, 20 m and 30 m. To include the whole range affected by groundwater movement, the side boundary of the model was chosen to be 200 m away from the tunnel centre, which is equivalent to 10 times the tunnel depth. The bottom boundary is located 50 m below the ground surface. The nonlinear elastic small strain model combined with the Mohr-Coulomb model were used to represent soil behaviour. The nonlinear elastic small strain response of the soil was represented by the model described by Jardine (1985) and Jardine *et al.* (1986). Permeability is the critical parameter governing the post-construction behaviour. A nonlinear permeability model proposed by Vaughan (1989)

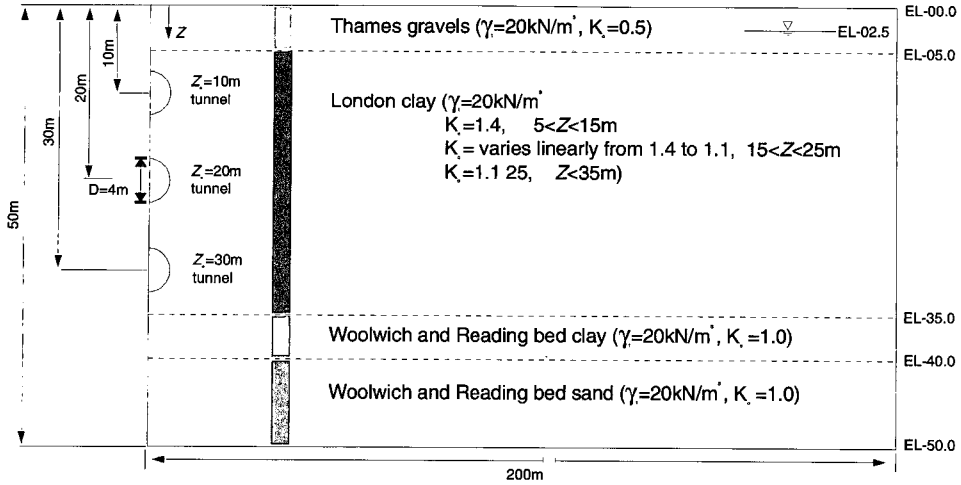

Fig. 6. Soil and tunnel profile

was used. The permeability function is used to reduce flow rate in the region between the initial and current phreatic surfaces. Approximate suction limit of 100 kPa is used. The lining segments are modelled with continuous linear elastic beam elements. The joints between the tunnel lining segments were not modelled and therefore the lining forms a continuous ring. The material parameters used are summarized in Appendix.

Initial and Boundary Conditions

This paper considers only the post-construction behaviour of the analyses performed. All analyses cases have the same initial volume loss of 2% inherited from construction which is the typical volume loss in long term London Clay. Only the fully permeable lining is considered and modelled by prescribing the pore water pressure on the excavation boundary as zero, i.e. p=0 for each increment.

A constant groundwater table and an impermeable excavation boundary condition were assumed during construction. 15 days were assigned for the simulation of the construction sequence. The Thames Gravel and Woolwich and Reading Bed sand are prescribed as fully drained non-consolidating materials, thus the pore water pressures in these soils were held constant for both the construction and the post-construction stages of the analyses.

As the monotonic consolidation is assumed in the analysis, further development of suction beyond prescribed shrinkage limit may cause unrealistic volume change above phreatic surface. Thus to avoid this unrealistic behaviour, the development of suction was monitored during the analysis. The fully permeable lining is modelled by prescribing the pore water pressure on the excavation boundary as zero. Meanwhile it is assumed that the pore water pressure at the far boundary keeps constant. At the surface of ground water, zero flow rate is prescribed for both confined and unconfined flow condition.

4. Results

The results were analysed by comparing flow patterns, ground behaviour and tunnel performance. Most results presented in this paper are for the long term steady state condition, if not stated otherwise.

4.1 Flow Behaviour

The variations of permeability around a tunnel were investigated using the nonlinear permeability model proposed by Vaughan (1989) where the permeability k, varies exponentially with the mean effective stress p, i.e. $k = k_o \exp(-Bp)$. The calculated permeability is presented and compared in Figure 7. Because of a low value of B (=0.007), the initial variation of k with depth is not significant. After completion of tunnel construction the permeability has not changed significantly except in the region very close to the tunnel as shown in Figure 7 (a). The permeability immediately adjacent to the tunnel increases, which corresponds to a decrease in mean

effective stress. The k values in the far field of the model present the pre-excavation ko values and have not changed during construction.

Under an unconfined flow condition the reduction in pore water pressure resulted in an increase in effective stress. Consequently, the soil around the tunnel has become less permeable as shown in Figure 7 (b). At the tunnel spring line k has slightly decreased from 1.3×10^{-10} m/s after construction to 9.5×10^{-11} m/s in the long-term. However, the development of pore water suctions above the phreatic surface has caused a slight increase in mean effective stress around the tunnel. Thus, the soil has become slightly less permeable. Scarcity of field data makes it difficult to compare the predicted results with observations.

Figure 8 presents flow nets under confined and unconfined flow conditions. Seven flow lines and seven equi-potential lines are presented for each flow net. The symmetric soil boundary along the tunnel center line is a flow line, and the boundary between consolidating and non-consolidating soil layers is equi-potential line. Comparing flow nets under unconfined flow conditions with those under confined flow conditions shows significant difference. Owing to the draw-down of the ground water table, a much larger zone of soil is affected by the flow of water. The development of suction above the phreatic surface has increased the pore water pressure head and resulted in changes to the position of the equi-potentials. Figure 9 shows the variation of pore water pressure under unconfined conditions and compares it with that of a confined flow condition. It is shown that pore water pressures for both cases decreased with time, and slightly higher pore water pressures were shown under a unconfined flow condition at steady state.

Figure 10 shows the phreatic surface at steady state conditions and compares the position of the phreatic surfaces at steady state for different tunnel depth. When the tunnel depth is 10 m, the phreatic surface reaches the tunnel. In the case where the tunnel depth is 20 m, the phreatic surface has been drawn down by 8 m. Up to a certain depth, the draw-down of the phreatic surface

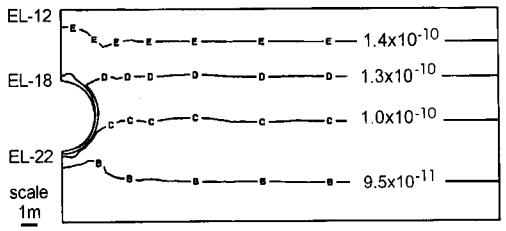

(a) after construction

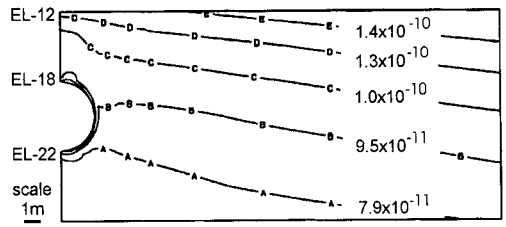

(b) Long-term condition under unconfined flow condition

Fig. 7. Variation of permeability adjacent to tunnel (m/sec)

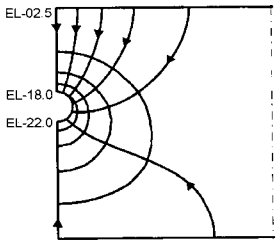

(a) confined flow

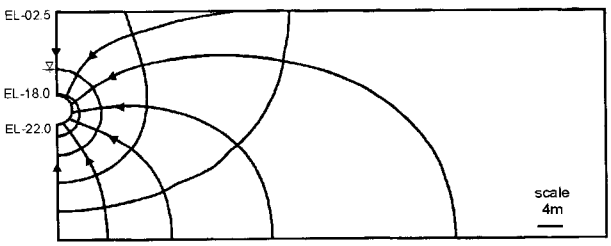

(b) unconfined flow

Fig. 8. Flow nets

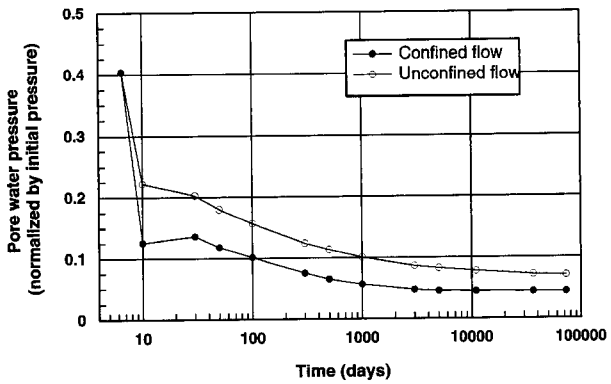

Fig. 9. Variation of pore water pressure with time (at tunnel crown)

seems to increase with tunnel depth. However, at the 30 m tunnel depth this draw down is smaller than for the 20 m tunnel depth. In this case, however, it should be noted that the drainage layer at 35 m may have a significant influence. These results are plotted in Figure 10 (a). Figure 10 (b) shows the draw-down of phreatic surface with tunnel depth at the tunnel center. It is interesting to note that there is a specific tunnel depth which gives maximum draw-down.

4.2 Ground Behaviour

To investigate the effect of draw-down of the phreatic surface, a comparison of ground behaviour between confined and unconfined flows is made. Figure 11 presents the volumetric strain, stress ratio and stress level at steady

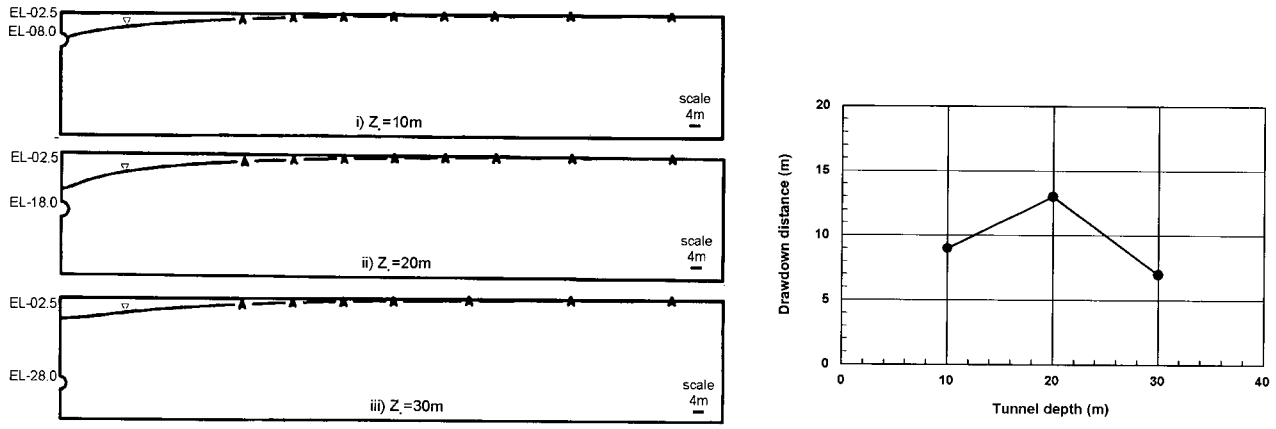

(a) phreatic surfaces with tunnel depth

(b) draw down and tunnel depth

Fig. 10. Prediction of phreatic surfaces

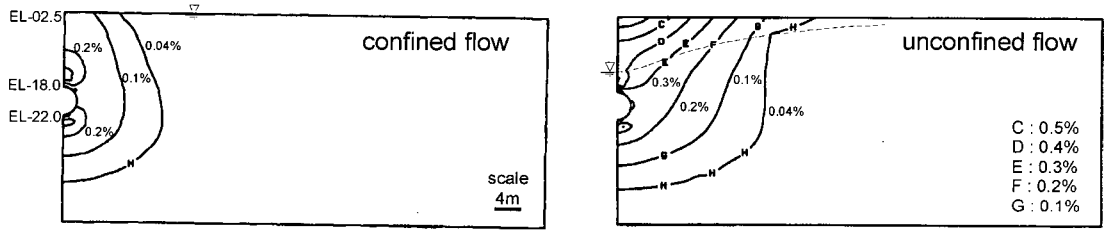

(a) volumetric strain

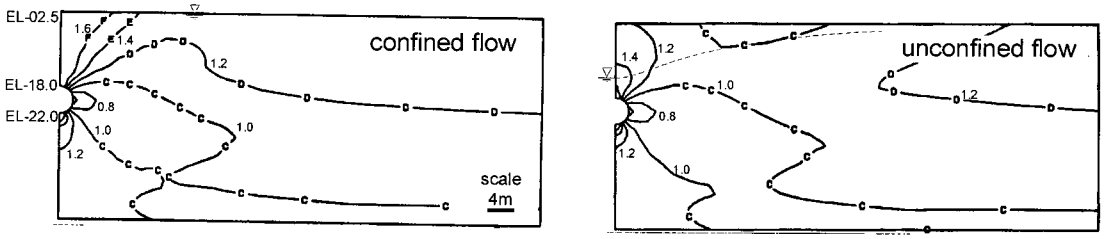

(b) stress ratio, σ_h/σ_v'

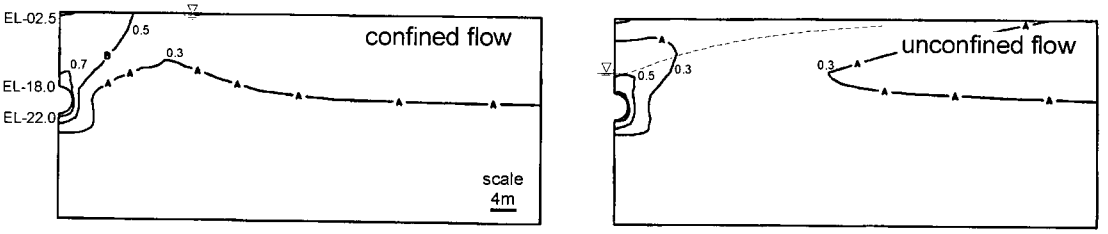

(c) stress level

Fig. 11. Ground behaviour for confined and unconfined flow conditions

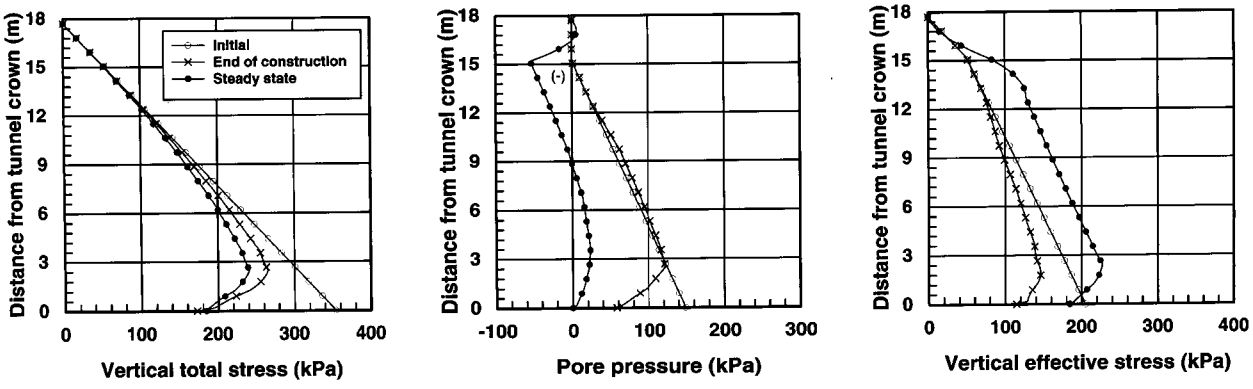

(a) vertical total stress (b) pore pressure (c) vertical effective stress

Fig. 12. Stress distribution above the tunnel crown under unconfined flow condition

state conditions for confined and unconfined flows. Considerable differences are found in the zone between the initial phreatic surface and the current phreatic surface. Large volumetric strains, a significant reduction in stress ratio and lower stress levels, but higher vertical effective stresses are observed in the case of unconfined flow compared to the case of confined flow. On the other hand, the ground behaviour below the current phreatic surface does not show any significant difference. Inspection of the stress distribution above the tunnel crown shows the influence of groundwater movements.

It would be interesting to investigate the detail of difference in ground behavior above tunnel crown between unconfined and confined flow. Figure 12 presents the stress distribution of ground for the unconfined flow condition. The maximum suction is about 60 kPa and develops at 2.5 m below the initial ground water table. The suction above the phreatic surface increases the effective vertical stress significantly. However, the resulting total stress has not changed significantly. An appreciable increase in effective vertical stress was obtained, but the total stress representing ground loading has hardly changed.

4.3 Lining Response

A slight increase in ground loading after a long period was obtained, which may reflect the effect of suction. The change of long term ground loading is not significant. Figure 13 (a) compares the distribution of ground loading on the tunnel lining. The ground loading on the lining is plotted in terms of percentage of overburden pressure. From a design point of view, the effect of draw-down of the water table is unlikely to cause any detrimental effect to the tunnel lining. Figure 13 (b) presents shear

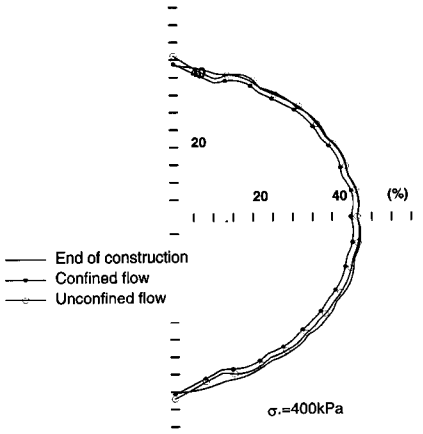

(a) as a percentage of overburden pressure

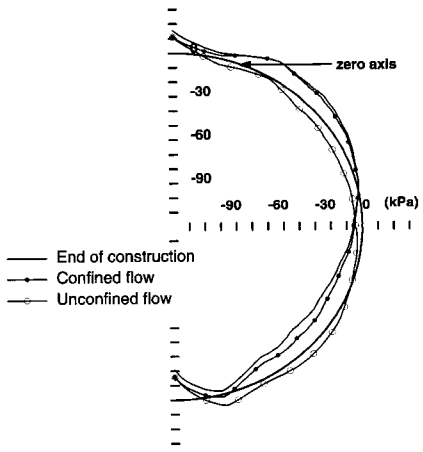

(b) distribution of shear stress on the tunnel lining

Fig. 13. Ground loadings and shear stresses on the lining

stresses between lining and soil.

Figure 14 shows the distribution of hoop thrust around the lining. The hoop thrust is about 45% of overburden at spring line. Figure 15 compares the long term movement. The tunnel experiences downwards movement. The long term tunnel movement depends on ground behaviour, rather than on the stresses in the lining, thus indicating a rigid body motion of the lining, i.e. consolidation behaviour in a soil causes the ground to subside, which results in downwards movement of the tunnel, while swelling of the soil causes the tunnel to move upwards.

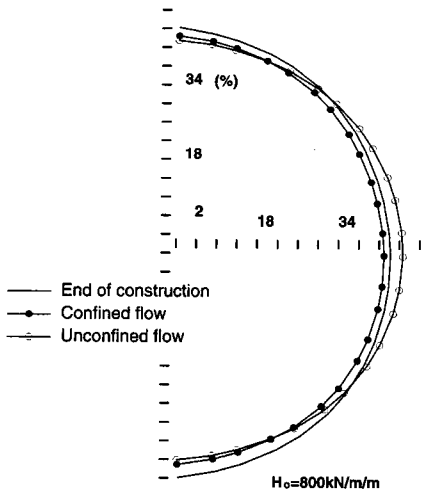

Fig. 14. Distribution of hoop thrusts

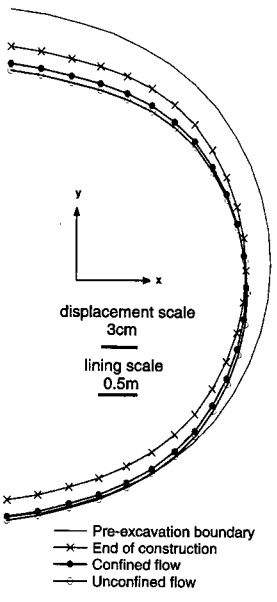

Fig. 15. Long term movement of tunnel lining

5. Discussions

Throughout this paper, it has been noted that there is considerable differences in ground behaviour depending on whether the flow is confined or unconfined particularly in soils above phreatic surface. In reality, however, the hydraulic boundary conditions are governed by the climate and the hydro-geophysical environment. As cyclic and transient effects can not be accurately simulated numerically, a simplification of monotonic consolidation is made for the analysis in this study. In practice, however, the actual hydraulic boundary conditions are rather complicated and mainly governed by climate. Evaporation and surrounding hydrology are also important factors. Conditions within the ground surface zone subjected to seasonal changes are complex. This cyclic effect can not be accurately modelled. To simplify this situation and avoid excess surface volume change due to the development of suction, pore water pressure change at the ground surface during analysis was prescribed as zero. The draw-down of the water table due to tunnel construction has been occasionally measured (Shirlaw *et al.*, 1996), but the development of suction and its effect have rarely been reported.

In this study the effect of the draw-down of the ground water table and the development of suction have been simulated by modeling monotonic consolidation and employing realistic permeability functions. Although this assumption may not produce the full surface effects experienced in the field (i.e. rainfall may reduce suction considerably), the results presented in this paper have indicated several interesting aspects associated with tunnelling below groundwater table.

6. Conclusions

Numerical formulation of unconfined flow was made, and successfully implemented into coupled finite element program. It is, however, noteworthy that, to consider the variation of permeability close to a tunnel it is necessary to have a fine mesh in that locality. When a coarse mesh is used around the tunnel, the reduction in mean effective stress and hence the increase in permeability could be

Appendix : Material parameters (Jong-ho Shin et al, 2002)

a. Small strain nonlinear elastic parameters

Shear modulus parameters	A	B	$C(\%)$	α	γ	$E_{d\,min}(\%)$	$E_{d\,max}$ (%)	G_{min} (kPa)
Thames Gravel	1104	1035	$5x10^{-4}$	0.974	0.940	$8.8334x10^{-4}$	0.3664	2000.0
London Clay	1400	1270	$1x10^{-4}$	1.335	0.617	$8.66025x10^{-4}$	0.6928	2666.7
W&R Beds Clay	1000	1045	$5x10^{-4}$	1.334	0.591	$13.8564x10^{-4}$	0.3811	2666.7
W&R Beds Sand	1300	1380	$1x10^{-4}$	1.220	0.649	$1.90526x10^{-4}$	0.1300	1000.0
Bulk modulus parameters	R	S	$T(\%)$	δ	λ	$\varepsilon_{v\,min}(\%)$	$\varepsilon_{v\,min}$ (%)	K_{min} (kPa)
Thames Gravel	275	225	$2x10^{-3}$	0.998	1.044	$2.1x10^{-3}$	0.20	5000
London Clay	686	633	$1.x10^{-3}$	2.069	0.420	$5.0x10^{-3}$	0.15	5000
W&R Beds Clay	530	460	$5x10^{-4}$	1.492	0.678	$1.5x10^{-3}$	0.16	5000
W&R Beds Sand	275	235	$5x10^{-4}$	1.658	0.535	$5.1x10^{-4}$	0.30	5000

b. Mohr-Coulomb yield parameters

Depth (m)	Soils	Cohesion intercept (kPa)	Angle of shearing resistance (°)	Angle of dilatancy (°)
0m to 5m	Thames Gravel	0	35	17.5
5m to 35m	London Clay	5	23	0
35m to 40m	W&R Beds Clay	25	27	0
40m~50m	W&R Beds Sand	0	34	17.5

c. Permeability models

Depth (m)	Soils	k_o (m/s)	$\beta(m^2/MN)$	p'_1	p'_2	R
0m to 5m	Thames Gravel	n/a	n/a	n/a		
5m to 35m	London Clay	$1.0.x10^{-10}$	0.007	50	100	100
35m to 40m	W&R Beds Clay	$1.0.x10^{-10}$	0.007	50	100	100
40m~50m	W&R Beds Sand	n/a	n/a	n/a		

d. Lining properties

	Area (m^2)	I (m^4)	E(kPa)	μ
Cast iron	0.168	0.00039514	$2.8\ x10^7$	0.15

missed.

The general effects of ground water movements on tunnel behaviour under unconfined flow condition were identified. The main features in comparison with those under confined flow conditions can be summarized as follows:

(a) A larger volume of soil is influenced and a longer time to reach steady state seepag equilibrium is required;

(b) The development of suction causes some volumetric reduction in the ground above the current phreatic surface;

(c) No significant difference in ground loading on the lining is seen for the confined and unconfined flow conditions. Conclusively, it can be stated that the draw-down of the water table may cause deeper and wider surface settlements, however, the effect of draw-down on the tunnel lining is negligible.

References

1. Barden, L. (1965), *Consolidation of compacted and unsaturated clays*, Geotechnique, Vol.15, No.3, pp.267-286.
2. Barratt, D.A. and Tyler, R.G. (1976), *Measurements of ground movements and lining behaviour on the London Underground at Regents Park.* Transport Road Research Laboratory Report 684.
3. Biot, M.A. (1941), *General theory of three dimensional consolidation*, J. Appl. Physics, Vol.12, pp.155-169.
4. Bowers, K.H., Hiller, D.M., and New, B.M. (1996), *Ground movement over three years at the Heathrow Express Trial Tunnel*, Proc. Int. Sym. on Geotechnical Aspects of Underground Construction in Soft Ground, London, pp.647-652.
5. Childs, E.C. and Collis-George, N. (1950), *The permeability of porous materials*, Proc. Royal society, Vol.51, No.2, pp.131-172.
6. Fredlund, D.G. (1997), *An introduction to unsaturated soil mechanics*, Unsaturated Soil Engineering Practice, Geotechnical Special Publication No.68, Logan, pp.1-37.
7. Fredlund, D.G., Xing, A., and Huang, S. (1994), *Predicting the permeability function for unsaturated soils using the soil water characteristics curve*, Can. Geotech. J., Vol.31, pp.533-546.
8. Freeze, R.A. and Cherry, J.A. (1979), *Groundwater*, Prentice-Hall.
9. Gardener, W.R. (1958), *Some steady-state solutions of the unsaturated moisture flow equation with application to evaporation from a water table*, Soil Science, Vol.85, pp.228-233.
10. Jardine, R.J., Potts, D.M., Fourie, A.B., and Burland, J.B. (1986), *Studies of the influence of nonlinear stress-strain characteristics in soil-structure interaction*, Geotechnique, Vol.36, No.3, pp.377-396.
11. Johnston, P.R. and Clough, G.W. (1983), *Development of a design technology for ground support for tunnels in soil*, Vol.1, U.S. Department of Transportation, Urban Mass Transportation Administration.
12. Jong-ho Shin, T.I. Addenbrooke, and D.M. Potts (2002), *A numerical study of the effect of groundwater movement on long term tunnel behaviour*, Geotechnique, Vol.52, No.6, pp.391-403.
13. Potts, D.M. and Zdravkovic, L. (1999), *Finite element analysis in geotechnical engineering, Theory*, Thomas Telford, London.
14. Shirlaw, J.N., Pennington B.N., and Yi X. (1996), *Monitoring during the construction of the Allen sewer tunnel*, Proc. Int. Sym. on Geotech. Aspects of Underground Construction in Soft Ground, London, pp.429-434.
15. Sparks, A.D.W. (1963), *Theoretical considerations of stress equations for partly saturated soils*, The 3rd Regional Conf. for Africa on Soil Mechanics and Foundation Engineering, Salisberg.
16. Toll, D.G. (1995), *A conceptual model for the drying and wetting of soil*, Proc. Conf. on Unsaturated Soil, Paris, pp.805-810.
17. Vaughan, P.R. (1989), *Non-linearity in seepage problems-Theory and field observation*, De Mello Volume, Sao Paulo, pp.501-516.

(received on Jun. 14, 2005, accepted on Aug. 16, 2005)